Modeling of disorder effects and optical extinction in three-dimensional photonic crystals

Luis A. Dorado and Ricardo A. Depine*
Departamento de Física, Grupo de Electromagnetismo Aplicado, Facultad de Ciencias Exactas y Naturales, Universidad de Buenos Aires, Ciudad Universitaria Pabellón I, C1428EHA Buenos Aires, Argentina
(Received 23 June 2008; revised manuscript received 4 November 2008; published 28 January 2009)

We present three different methods for the modeling of disorder effects in three-dimensional photonic crystals. In order to reproduce experimental results, we apply a method based on a statistical distribution of sphere sizes and vacancy density in a colloidal crystal slab. The other two methods consist of adding extinction to the theoretical model so energy losses account for the diffuse light scattering produced by imperfections in the crystalline structure, which removes energy from coherently scattered waves. Although we exemplify the case of synthetic opals, our analysis also applies to other kinds of photonic crystals.

DOI: 10.1103/PhysRevB.79.045124 PACS number(s): 42.70.Qs, 42.25.Dd, 78.40.−q, 78.20.Bh

I. INTRODUCTION

Three-dimensional (3D) photonic crystals (PCs) have attracted much attention during the last decades mainly due to the possibility of an intelligent control of light and the potential applications in optoelectronics and microwave devices.[1,2] Spatial periodicity of the dielectric function along three independent directions is essential in order to obtain a complete band gap where the propagation of light along any direction is forbidden for photon energies within the gap.[3,4] The need for simple and fast methods of fabricating 3D PCs with band gaps in the near-infrared and visible spectra has lead to the use of colloidal particles in the micrometer scale. Hence, fabrication methods that take advantage of the self-assembling properties of dielectric spheres are now available and their permanent improvement has produced colloidal PCs with a low degree of defects.[5–9] In this paper we are interested in unintentional disruptions that arise in the spatial periodicity during the fabrication process.[10–16] These intrinsic defects or imperfections are different from local defects, which are introduced by adding or removing materials in a controlled manner in order to achieve localized modes within the band gaps[17,18] in analogy with the doping of semiconductors.[19] In the low-energy range, where the lattice constant is less than the wavelength of light, the size of imperfections in the crystalline structure is small compared to the wavelength. Thus, in this range, the optical response of the real PC, although slightly modified, is basically that of a perfectly ordered one.[20] However, in the high-energy range[21] where the lattice constant is greater than the wavelength, the size of defects becomes important and the optical spectra of a real PC are very different from those of a perfect one.[20,22–24] Therefore, the reproduction of experimental reflectance and transmittance spectra via any theoretical approach requires the modeling of disorder in some way.

Deviations from perfect periodicity cause scattering and hence exponential attenuation of the coherent radiation propagating through a PC. In the low-energy range the degree of disorder has been evaluated using the concept of extinction length[13] or assigning an imaginary part to an effective refractive index.[14] A rather different approach has been recently used to reproduce optical features observed for colloidal crystals in the high-energy region.[20,22–24] In this approach, disorder effects observed in spherical colloidal crystals made of *lossless* materials have been satisfactorily modeled by keeping the hypothesis that the spheres are arranged in a perfectly periodic lattice while introducing some loss via the imaginary part of the dielectric constant of the latex spheres. Excellent agreement with different experimental results has been obtained although latex absorption is known to be negligible in the considered spectral range. In particular, the approach has been used to explain why a very fine-featured theoretically expected reflection spectrum[25]—due to the complicated band structure of the high-energy region—has not been experimentally observed yet.[20] Moreover, the imaginary dielectric constant introduced into the model has been shown to be a function of the crystal size, which indicates that this single parameter can be used as a measure of the degree of disorder in a real PC slab.[22] The approach has also been used to explain the physical origin of reflectance and transmittance features observed in the high-energy range[23] and to reproduce the spectra of nonspecular spots diffracted from colloidal crystals.[24]

The results obtained with the extinction method indicate that the introduction of losses to model PCs with lossless building blocks can be regarded as a convenient theoretical tool to account for diffusely scattered light produced by disorder and imperfections, a mechanism which removes energy from the specularly reflected and forward transmitted beams. However, this approximation, although useful to fit experimental results, does not seem to be completely satisfactory from a physical point of view. Many quantitative and qualitative questions remain to be answered, such as whether the effect of imperfections can be distinguished from actual absorption within a PC building block, how different types of imperfections contribute to the imaginary part of the dielectric constant, or whether there is a unique way to represent a variety of imperfections by a single extinction parameter.

The purpose of this paper is to address some of these questions using the electromagnetic counterpart of one of the simplest approximations used in the electron-scattering problem:[26,27] the average T-matrix approximation (ATA). In the ATA method—generally valid when the disorder is weak—the scattering matrix (T-matrix) of a single scatterer is averaged over particle states obtaining a sort of average scatterer, and the actual disordered structure is replaced by a perfectly periodic lattice of this average scatterer. In the PC

version, particle states refer to distributions of size, shape, position, orientation, refractive index, etc., of the scatterers, so we will employ statistical methods in order to calculate the ATA matrix.[28] Electromagnetic interactions between the scatterers arranged in a periodic lattice will be calculated by means of the layer-multiple-scattering method for spherical scatterers,[29–32] usually known as the vector version of the Korringa-Kohn-Rostoker (KKR) method.[33] For the sake of simplicity, we assume that the scatterers are homogeneous spheres, although KKR methods can be, in principle, extended to other systems of spherical and nonspherical particles, because the scattering properties of the individual scatterers enter only through the corresponding T matrix.[34,35]

Some previous uses of the ATA for the evaluation of disorder effects in PCs include systems of metallic spheres[30,36] and studies on negative refraction in random photonic alloys of polaritonic and plasmonic microspheres.[37] ATA results have also been used as a reasonable initial input for iterative schemes obtained in the frame of improved treatments of disorder based on the so-called coherent-potential approximation.[38] Here we use the ATA method to evaluate disorder effects in 3D PCs constructed from *intrinsically transparent* building blocks. We exemplify the case of synthetic opals, but our analysis also applies to other kinds of PCs. Among all the sources of unavoidable imperfections, we focus on those originating from a statistical distribution of sphere sizes and vacancy density. Our results show that a fairly good fitting of experimental curves can be obtained when these two kinds of defects are taken into account.

This paper is organized as follows. In Sec. II the use of the ATA method within the framework of the KKR multiple-scattering approach for spherical particles is reviewed. The focus of the formulation is placed on disorder effects related with polydispersity[39] or variations in the size of particles as well as sphere vacancies. In Sec. III we present numerical results obtained with the ATA method and compare our simulations with the experimental spectra reported by two independent research groups.[9,21] A very good agreement, previously obtained only with the extinction approach, is observed between theory and experiment. Some ideas of the ATA method are used in Sec. IV to obtain more flexible versions of the simple extinction approach in which the effect of imperfections is managed through the use of two, instead of one, parameters. Finally, in Sec. V, the more outstanding results are summarized and discussed.

II. ATA-KKR METHOD FOR MODELING DEFECTS

We begin with a brief description of the scattering by a single sphere and the calculations involved in the vector KKR method.[29–32] An incident electromagnetic wave on a sphere centered at the origin of coordinates ($\vec{r}=0$) has an electric field with a spherical wave expansion given by[40]

$$\vec{E}(\vec{r}) = \sum_{l=1}^{\infty} \sum_{m=-l}^{l} \left[\frac{i}{k} a_{lm}^{0E} \vec{\nabla} \times j_l(kr) \vec{X}_{lm}(\theta,\phi) + a_{lm}^{0H} j_l(kr) \vec{X}_{lm}(\theta,\phi) \right], \quad (1)$$

where (r,θ,ϕ) are the usual spherical coordinates of an evaluation point $\vec{r}$, ϵ and μ are the dielectric permittivity and magnetic permeability, respectively, of the homogeneous medium outside the sphere, ω is the angular frequency, c is the velocity of light in vacuum, $k=\sqrt{\mu\epsilon}\omega/c$, $j_l(kr)$ are the spherical Bessel functions of the first kind, and $\vec{X}_{lm}(\theta,\phi)$ are the vector spherical harmonics. The magnetic field can be obtained from Maxwell's equations and has a similar series expansion. In this multipole expansion, the integers (l,m), where $l \geq 1$ and $-l \leq m \leq l$, represent a spherical partial wave of order (l,m), which can be either electric (with complex amplitude a_{lm}^{0E}) or magnetic (with complex amplitude a_{lm}^{0H}). Dipole fields correspond to $l=1$, quadrupole fields correspond to $l=2$, and so on. By applying the orthogonality property of the vector spherical harmonics, it is straightforward to prove that electric multipoles radiate transverse magnetic (TM) fields, while magnetic multipoles radiate transverse electric (TE) fields. Thus, the multipole expansion in Eq. (1) can also be viewed as a linear combination of TM and TE spherical waves. In a numerical calculation, a cut-off LMAX in the multipole expansion must be chosen, retaining the first 2 LMAX (LMAX+2) terms. The electromagnetic field scattered by the sphere at the origin is given by replacing $j_l(kr)$ with the spherical Hankel function of the first kind $h_l^+(kr)$, which corresponds to outgoing spherical waves. Also, the coefficients a_{lm}^{0P} must be replaced with the new coefficients a_{lm}^{+P} of the scattered wave, where $P=E,H$. The T-matrix $\mathbf{T}$ relating the incident and scattered wave coefficients, a_{lm}^{0P} and a_{lm}^{+P}, can be found by enforcing the boundary conditions on the surface of the sphere. It can be proved[32] that this matrix is diagonal, $\mathbf{T}=T_l^P \delta_{PP'} \delta_{ll'} \delta_{mm'}$, and that its elements are given by

$$T_l^E = \left[\frac{j_l(k_s r) \frac{\partial}{\partial r}[r j_l(kr)] \epsilon_s - j_l(kr) \frac{\partial}{\partial r}[r j_l(k_s r)] \epsilon}{h_l^+(kr) \frac{\partial}{\partial r}[r j_l(k_s r)] \epsilon - j_l(k_s r) \frac{\partial}{\partial r}[r h_l^+(kr)] \epsilon_s} \right]_{r=S}, \quad (2)$$

where S is the sphere radius, ϵ_s and μ_s are the dielectric permittivity and magnetic permeability of the sphere, and $k_s=\sqrt{\mu_s \epsilon_s}\omega/c$. The matrix elements T_l^H can be obtained from Eq. (2) by means of the transformations $\epsilon_s \leftrightarrow \mu_s$ and $\epsilon \leftrightarrow \mu$.

Once the T matrix of a single sphere has been obtained, the multiple scattering between identical spheres arranged in a given periodic lattice can be calculated by means of the vector KKR method. In the layer version of this method,[31] the 3D PC slab is first divided into layers parallel to a given crystallographic plane and the multipole expansion in spherical waves is used to account for the multiple-scattering process inside a layer. Next, a series expansion in a plane-wave basis is used to calculate the electromagnetic interactions between layers and to compute the far-field power flux in both sides of the crystal slab.

The scatterers composing a real colloidal PC are generally not perfectly spherical, having size and shape distributions over an ensemble of scatterers. Moreover, the scatterers are not located at sites of a perfectly periodic lattice. All these imperfections in the crystalline structure of a real PC pro-

duce diffuse light scattering, which removes energy from the coherently scattered waves. If there are N types of scatterers with different T matrices $\mathbf{T}_i$, $i=1,2,\ldots,N$, each of these scatterers is replaced in the ATA method with a single average scatterer described by an average T matrix given by

$$\langle \mathbf{T} \rangle = \sum_{i=1}^{N} C_i \mathbf{T}_i, \tag{3}$$

where C_i is the concentration of the ith scatterer and $\Sigma_{i=1}^{N} C_i = 1$. Since each lattice site is occupied by an average scatterer, the application of the KKR method proceeds in the same fashion as in the case of ordered PC slabs. The ATA method can also be applied for the modeling of vacancies.[38] For example, if $C \leq 1$ denotes the fraction of lattice sites occupied by identical scatterers described by a T matrix $\mathbf{T}$ and the remaining $1-C$ sites are empty, then Eq. (3) reduces to $\langle \mathbf{T} \rangle = C\mathbf{T}$.

The ATA method can be extended for the case of a continuous distribution of scatterer types. As a first approximation, we could consider that the distributions of size, shape, position, orientation, refractive index, etc., of the scatterers are statistically independent from each other when their deviations from the mean values are small enough.[28] Under this condition, we will focus our interest on the effect of the size distribution of spheres centered at lattice sites. Assuming that the radii s are distributed according to a random process with probability density function $P(s)$, the average T matrix in Eq. (3) is given by

$$\langle \mathbf{T} \rangle = \int \mathbf{T}(s) P(s) ds. \tag{4}$$

Besides, if vacancies (concentration $1-C$) are included, the spheres of the statistical ensemble can only be centered at a fraction C of the lattice sites. In this case, we see that Eq. (3) becomes

$$\langle \mathbf{T} \rangle = C \int \mathbf{T}(s) P(s) ds. \tag{5}$$

Similar expressions can be obtained whenever disorder effects associated with vacancies and with a continuous size distribution of scatterers are separated from other sources of disorder. In this study we will assume a Gaussian distribution $P(s)$ of sphere radii with mean S_{av} (average radius) and standard deviation σ since the theoretical results obtained through this approach are compatible with measurements reported in the literature. Also, in the limit of small degrees of disorder, that is, when $\sigma \ll S_{\mathrm{av}}$, the results and conclusions obtained from the Gaussian distribution are basically the same as those obtained from other probability density functions, e.g., logarithmic normal, gamma, and modified gamma distributions.[28]

III. ATA RESULTS

The model structure we will employ for our analysis is a close-packed face-centered-cubic (fcc) lattice of spheres of dielectric constant $\epsilon_s = 2.5$ embedded in a medium of $\epsilon = 1$,

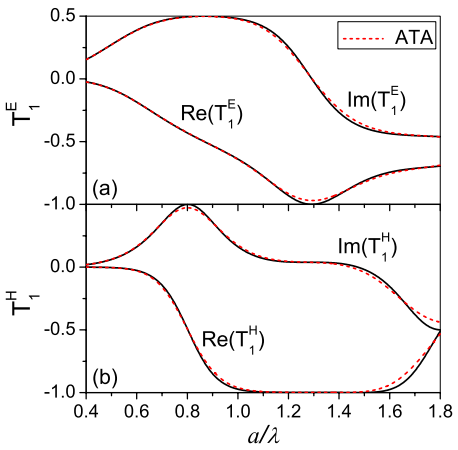

FIG. 1. (Color online) Real and imaginary parts of the single-sphere scattering coefficients corresponding to: (a) electric dipoles (T_1^E) and (b) magnetic dipoles (T_1^H) for a sphere dielectric constant $\epsilon_s = 2.5$. Solid lines correspond to a sphere radius $S = 0.5a$ and dashed lines correspond to ATA with an average radius $S_{\mathrm{av}} = 0.5a$ and standard deviation $\sigma = 0.05 S_{\mathrm{av}}$.

which corresponds to latex spheres in air. This structure has been repeatedly fabricated and measurements of its reflectance and transmittance spectra are available in the literature.[5] The crystal growth direction is typically [111],[6] so we will focus on the optical response when an incident light beam impinges in that particular direction (normal incidence). The photon energy is expressed in reduced units a/λ, where a is the lattice constant of the classical cubic cell and λ is the wavelength of the incident light. In the case of a Gaussian distribution, the integral in Eq. (4) extends over an infinite interval and cannot be solved in closed form, so an iterative Romberg's quadrature[41] routine has been used to perform the integrations numerically. Also, a spherical wave expansion cutoff LMAX=9 and 41 plane waves[31,32] have been used in the vector KKR method in order to obtain converged results for the reflectance and transmittance coefficients, R_{00} and T_{00}, in the range of energies we are interested in.

The main multipole field scattered by the spheres in the lattice is the dipole field ($l=1$), then the T-matrix elements corresponding to electric and magnetic dipoles are T_1^E and T_1^H, respectively. In Fig. 1, the real and imaginary parts of these dipolar elements are plotted as functions of the reduced photon energy. Solid lines are the results obtained directly from Eq. (2) for a single sphere with radius $0.5a$, while dashed lines correspond to the ATA matrix obtained for an ensemble of spheres characterized by $S_{\mathrm{av}} = 0.5a$ and $\sigma/S_{\mathrm{av}} = 0.05$, that is, a standard deviation of 5% from the mean radius. Due to the low standard deviation introduced, the single sphere and the average T matrices exhibit relatively small differences. However, we will see below that even smaller amounts of disorder have a tremendous effect on the ATA predicted response, especially in the high-energy range ($a/\lambda \geq 1$).

In Fig. 2(a) we show the calculated reflectance spectrum of a close-packed perfectly periodic crystal, that is, $S_{\mathrm{av}} = 0.5a$ and $\sigma/S_{\mathrm{av}} = 0$. The spectrum exhibits a peak at a/λ

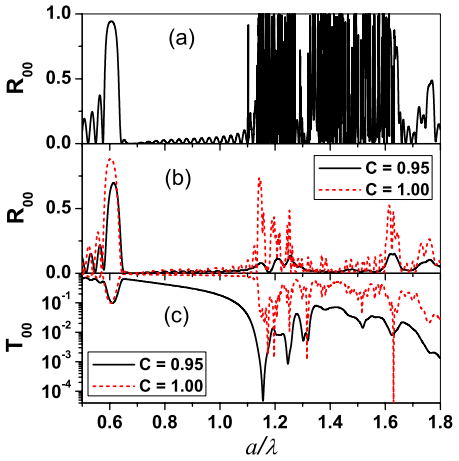

FIG. 2. (Color online) (a) Reflectance spectrum for a perfect crystal 18 layers wide with spheres of dielectric constant $\epsilon_s=2.5$ in air. (b) Reflectance and (c) transmittance spectra with ATA parameters: $S_{av}=0.5a$, $\sigma=0.05S_{av}$, $C=0.95$ (solid lines), and $C=1$ (dashed lines).

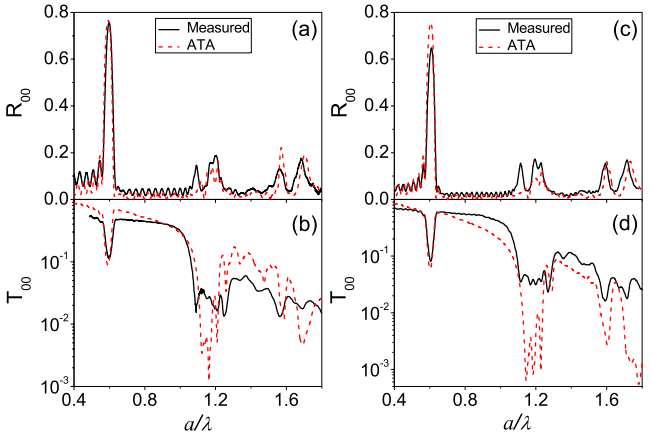

FIG. 3. (Color online) [(a) and (b)] Measured reflectance and transmittance spectra (solid lines) extracted from Ref. 9 for a crystal 18 layers wide and the calculated spectra (dashed lines) for spheres of dielectric constant $\epsilon_s=2.6$ in air and ATA parameters: $S_{av}=0.5a$, $\sigma=0.025S_{av}$, and $C=0.97$. [(c) and (d)] Measured reflectance and transmittance spectra (solid lines) extracted from Ref. 21 for a crystal 21 layers wide and the calculated spectra (dashed lines) for spheres of dielectric constant $\epsilon_s=2.5$ in air and ATA parameters $S_{av}=0.5a$, $\sigma=0.025S_{av}$, and $C=0.96$.

$=0.61$ due to the existence of a pseudo-band-gap in the photonic band structure and the usual Fabry-Pérot oscillations related to the finite thickness of the slab. In the high-energy range, an abruptly fluctuating behavior of the reflectance can be seen with several high peaks of unitary amplitude. As in the case of sphere monolayers,[42,43] these peaks arise from internal resonances of the PC that can be classified according to the main multipole interactions involved in the response of the system.[23] In Fig. 2(b), the reflectance spectrum has been recalculated for $\sigma/S_{av}=0.025$ and two different concentrations of vacancies. In the case of zero vacancies ($C=1$, dashed line) and within the low-energy range, the reflectance is basically the same as that shown in Fig. 2(a), which means that a small degree of disorder has little effect on the optical response for these low energies. However, the spectrum changes dramatically in the high-energy range, where the reflectance values have decreased significantly and several peaks have practically disappeared. By adding 5% of vacancies ($C=0.95$, solid line), the reflectance decreases even more and several peaks are smoothed out. In this case, only three peaks around $a/\lambda=1.2$ and two peaks above $a/\lambda=1.6$ can be observed. The transmittance spectrum plotted in Fig. 2(c) shows the same trend.

Although very fine-featured reflection spectra as that shown in Fig. 2(a) have not been experimentally reported yet to the authors' knowledge, the optical spectra in Figs. 2(b) and 2(c) are quite similar to measurements published in the literature. In Fig. 3 we compare the ATA results with spectra reported by two independent research groups: Figs. 3(a) and 3(b) correspond to Ref. 9, whereas Figs. 3(c) and 3(d) correspond to Ref. 21. Figures 3(a) and 3(b) show the comparison between the measured reflectance and transmittance spectra[9] (solid lines) and the spectra we calculated (dashed lines) for a PC 18 layers wide. The ATA parameters are $C=0.97$, $S_{av}=0.5a$, and $\sigma=0.025S_{av}$ whereas the best fitting value for the sphere dielectric constant is $\epsilon_s=2.6$. Analogously, Figs. 3(c) and 3(d) show the comparison between measured spectra[21] (solid lines) and our calculations (dashed lines) for a PC 21 layers wide, $\epsilon_s=2.5$, and ATA parameters $C=0.96$, $S_{av}=0.5a$, and $\sigma=0.025S_{av}$. A very good agreement between theory and experiment is observed in all cases. It is worth mentioning that this kind of agreement in the high-energy range had not been previously obtained by any other method except by adding extinction to the dielectric constant of the spheres.

From the results presented in Figs. 2 and 3 we realize that the inclusion of vacancies seems to be essential to reproduce experimental curves in the high-energy range. While the inclusion of dispersion in sphere radii attenuates several sharp resonances of the perfect lattice, the inclusion of empty sites in the lattice seems to produce a smoothing effect on the optical spectra. In Fig. 4 we show the optical spectra obtained with the ATA for $C=0.95$ and various values of σ/S_{av}. We can observe that reflectance peaks are attenuated as σ/S_{av} increases, while transmittance dips become more pronounced.

IV. EXTINCTION APPROACHES

In the inner extinction approximation (IEA) method a great variety of imperfections is represented by a single parameter via the imaginary part of the dielectric constant of the latex spheres. Analogously to the IEA, another single-parameter extinction approach to account for the diffusely scattered light that is removed from coherent beams could be envisaged. In this rather complementary approach, which will be referred to as the outer extinction approximation (OEA) method, the energy-loss mechanism is provided by a nonzero imaginary part of the dielectric constant ϵ of the medium surrounding the spheres, instead of being provided by a nonzero imaginary part of the dielectric constant ϵ_s of the latex spheres. Although for the case of latex spheres in air

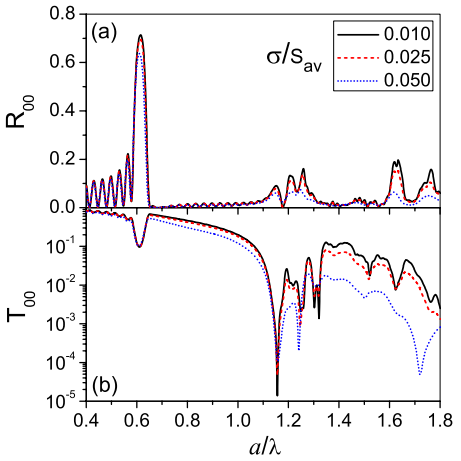

FIG. 4. (Color online) (a) Reflectance and (b) transmittance spectra for a crystal 18 layers wide with spheres of dielectric constant $\epsilon_s=2.5$ in air. The ATA parameters are: $S_{av}=0.5a$, $C=0.95$, and the spectra are shown for different values of σ/S_{av}.

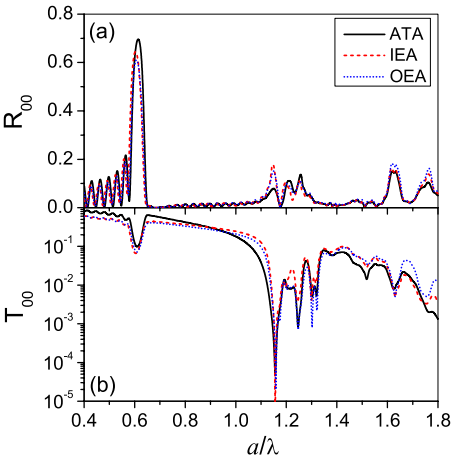

FIG. 5. (Color online) Comparison among the ATA, IEA, and OEA (a) reflectance and (b) transmittance spectra for a crystal 18 layers wide. ATA parameters: $\epsilon_s=2.5$, $\epsilon=1$, $S_{av}=0.5a$, $\sigma=0.025S_{av}$, and $C=0.95$. IEA parameters: $\epsilon_s=2.5+i0.04$, $\epsilon=1$, and $C=1$. OEA parameters: $\epsilon_s=2.5$, $\epsilon=1+i0.04$, and $C=0.97$.

the reader could feel more comfortable when latex and not air is to be considered the lossy medium, both extinction approximations are equivalent from a modeling point of view, and we have checked that both the IEA and OEA methods provide similar fittings of experimental curves. On the other hand, and in contrast with these single-parameter approaches, we have seen that the use of the ATA method allowed us to include different sources of deviation from perfect periodicity, represented in our previous examples by different parameters such as σ, S_{av}, or C. Taking into account that (i) both the IEA and OEA are computationally less demanding than the ATA and (ii) vacancies seem to play an important role in the optical response of self-assembling opal samples that are being produced nowadays, we have sought an improved method which, as in the ATA approach, incorporates the parameter $1-C$ representing the concentration of vacancies while avoiding, as in the extinction approaches, direct computation of the average T matrix demanded by the ATA method. The improvement can be achieved by noting that when vacancies are considered to be the only source of disorder, that is, when we assume that only a fraction $C<1$ of lattice sites is occupied by identical scatterers described by the same T matrix $\mathbf{T}$, then the average T matrix adopts the very simple form,

$$\langle \mathbf{T} \rangle = C\mathbf{T}. \tag{6}$$

If we are using the ATA method to obtain the optical response of a PC affected by vacancies as the only source of disorder, the calculation of the average T matrix $\langle \mathbf{T} \rangle$ does not require further explicit statistical calculations. Unfortunately, the convenient form of Eq. (6) must be abandoned and explicit statistical calculations—as those performed to obtain the results presented in Sec. III—are required for real samples affected not only by vacancies but also by other deviations from perfect periodicity. It is clear that for a PC constructed from lossless building blocks, real dielectric constants are to be used for the calculation of the scattering matrix $\mathbf{T}$ in Eq. (5) or (6). However, we could keep the convenient form of Eq. (6) for a PC affected only by vacancies if all the remaining deviations from perfect periodicity are assigned to extinction through the introduction, as in the IEA or OEA methods, of nonzero imaginary parts for the dielectric constants of the PC building blocks. By doing so, we can obtain more flexible versions of the simple extinction approach where the effect of imperfections is managed through the use of two, instead of one, parameters. Although it is not our purpose to investigate here how each parameter affects the reflectance and transmittance spectra, some hints can be obtained by the ATA results presented in Figs. 2 and 3, where the inclusion of dispersion in sphere radii seemed to attenuate several sharp resonances of the perfect lattice, while the inclusion of vacancies seemed to produce a smoothing effect on the optical spectra, but the question remains whether the effect of vacancies can be distinguished from the effect of other kind of imperfections by only measuring reflectance and transmittance spectra.

IEA, OEA, and ATA approaches are useful theoretical tools for reproducing the optical response of weakly disordered PCs. They all provide very good fittings of experimental data and essentially the same results when the disorder parameters are properly chosen. This can be observed in Fig. 5 where we have compared IEA, OEA, and ATA methods for the close-packed fcc lattice of spheres of dielectric constant $\epsilon_s=2.5$ embedded in a medium of $\epsilon=1$. To simulate disorder effects with the IEA method we have added an imaginary part to the dielectric constant of the spheres ($\epsilon_s=2.5+0.04i$), and no vacancies ($C=1$) have been introduced, while in the OEA method the same value of the imaginary part has been added to the outer dielectric constant ($\epsilon=1+0.04i$) but 3% of vacancies have been included ($C=0.97$). For the ATA method we have used $S_{av}=0.5a$, $\sigma=0.025S_{av}$, and $C=0.95$.

The close agreement between experiment, the ATA method, and the extinction approaches indicates that the reflectance and transmittance spectra of a 3D colloidal PC in the high-energy range are almost determined by the optical

extinction due to imperfections and defects in the crystalline structure of the slab.[20] These results would also indicate that a perfect PC with material absorption generates almost the same reflectance and transmittance as a disordered PC without material loss, however more experimental work is needed since we have made only a theoretical prediction in this case. Besides, we must point out that these results are valid when no diffracted beams emerge from the PC slab,[44] which would provide a mean to distinguish between different sources of disorder and losses in higher-energy ranges.

V. CONCLUSION

In summary, we have used the average T-matrix approximation to evaluate disorder effects in the optical response of photonic crystals. The ATA method has been applied to colloidal crystals and validated with experimental data available in the literature. Our numerical results show that disorder has little effect on the optical spectra in the low-energy range but affects dramatically the response of the system in the high-energy range. A very good agreement, in the high-energy range previously obtained only with the IEA method, is observed between theory and experiment. Using some ideas of the ATA method, we have shown how to obtain more flexible extinction approaches in which the effect of imperfections is managed through the use of two, instead of one, parameters. We have obtained a close agreement between experimental data and the results of the ATA method in the case of disordered photonic crystals with negligible material loss. Although this is also true for extinction methods, more experimental work on weakly disordered crystals with a certain amount of material loss is needed in order to demonstrate the usefulness of the ATA and extinction methods in these cases.

ACKNOWLEDGMENTS

The authors gratefully acknowledge stimulating discussions with H. Míguez. This work was supported by grants from Consejo Nacional de Investigaciones Científicas y Técnicas (CONICET), Agencia Nacional de Promoción Científica y Tecnológica (Contract No. PICT-11–1785), and Universidad de Buenos Aires (Contract No. X062).

*rdep@df.uba.ar

[1] E. Yablonovitch, Phys. Rev. Lett. **58**, 2059 (1987).
[2] K. Sakoda, *Optical Properties of Photonic Crystals* (Springer-Verlag, Berlin, Heidelberg, 2001).
[3] J. D. Joannopoulos, R. D. Meade, and J. N. Winn, *Photonic Crystals* (Princeton University Press, Princeton, NJ, 1995).
[4] K. M. Ho, C. T. Chan, and C. M. Soukoulis, Phys. Rev. Lett. **65**, 3152 (1990).
[5] J. F. Bertone, P. Jiang, K. S. Hwang, D. M. Mittleman, and V. L. Colvin, Phys. Rev. Lett. **83**, 300 (1999).
[6] P. Jiang, J. F. Bertone, K. S. Hwang, and V. L. Colvin, Chem. Mater. **11**, 2132 (1999).
[7] S. Wong, V. Kitaev, and G. A. Ozin, J. Am. Chem. Soc. **125**, 15589 (2003).
[8] K. Wostyn, Y. Zhao, B. Yee, K. Clays, A. Persoons, G. de Schaetzen, and L. Hellemans, J. Chem. Phys. **118**, 10752 (2003).
[9] H. Míguez, V. Kitaev, and G. A. Ozin, Appl. Phys. Lett. **84**, 1239 (2004).
[10] Z.-Y. Li and Z.-Q. Zhang, Phys. Rev. B **62**, 1516 (2000).
[11] V. N. Astratov, A. M. Adawi, S. Fricker, M. S. Skolnick, D. M. Whittaker, and P. N. Pusey, Phys. Rev. B **66**, 165215 (2002).
[12] M. Allard and E. H. Sargent, Appl. Phys. Lett. **85**, 5887 (2004).
[13] A. F. Koenderink, A. Lagendijk, and W. L. Vos, Phys. Rev. B **72**, 153102 (2005).
[14] J. F. Galisteo-López, M. Galli, M. Patrini, A. Balestreri, L. C. Andreani, and C. López, Phys. Rev. B **73**, 125103 (2006).
[15] R. Rengarajan, D. Mittleman, C. Rich, and V. Colvin, Phys. Rev. E **71**, 016615 (2005).
[16] G. Lozano and H. Míguez, Appl. Phys. Lett. **92**, 091904 (2008).
[17] P. V. Braun, S. A. Rinne, and F. García-Santamaría, Adv. Mater. (Weinheim, Ger.) **18**, 2665 (2006).
[18] A. Arsenault, F. Fleischhaker, G. von Freymann, V. Kitaev, H. Míguez, A. Mihi, N. Tetreault, E. Vekris, I. Manners, S. Aitchison, D. Perovic, and G. A. Ozin, Adv. Mater. (Weinheim, Ger.) **18**, 2779 (2006).
[19] E. Yablonovitch, T. J. Gmitter, R. D. Meade, A. M. Rappe, K. D. Brommer, and J. D. Joannopoulos, Phys. Rev. Lett. **67**, 3380 (1991).
[20] L. A. Dorado, R. A. Depine, and H. Míguez, Phys. Rev. B **75**, 241101(R) (2007).
[21] J. F. Galisteo-López and C. López, Phys. Rev. B **70**, 035108 (2004).
[22] L. A. Dorado, R. A. Depine, G. Lozano, and H. Míguez, Phys. Rev. B **76**, 245103 (2007).
[23] L. A. Dorado, R. A. Depine, G. Lozano, and H. Míguez, Opt. Express **15**, 17754 (2007).
[24] L. A. Dorado, R. A. Depine, D. Schinca, G. Lozano, and H. Míguez, Phys. Rev. B **78**, 075102 (2008).
[25] A. Modinos, N. Stefanou, and V. Yannopapas, Opt. Express **8**, 197 (2001).
[26] J. L. Beeby, Proc. R. Soc. London, Ser. A **279**, 82 (1964).
[27] J. L. Beeby, J. Phys. C **1**, 82 (1968).
[28] M. I. Mishchenko, L. D. Travis, and A. A. Lacis, *Multiple Scattering of Light by Particles* (Cambridge University Press, Cambridge, 2006).
[29] K. Ohtaka, J. Phys. C **13**, 667 (1980).
[30] A. Modinos, Physica A **141**, 575 (1987).
[31] N. Stefanou, V. Karathanos, and A. Modinos, J. Phys.: Condens. Matter **4**, 7389 (1992).
[32] N. Stefanou, V. Yannopapas, and A. Modinos, Comput. Phys. Commun. **113**, 49 (1998); **132**, 189 (2000).
[33] J. Korringa, Physica (Amsterdam) **13**, 392 (1947); W. Kohn and N. Rostoker, Phys. Rev. **94**, 1111 (1954).
[34] K. P. Velikov, A. Moroz, and A. van Blaaderen, Appl. Phys. Lett. **80**, 49 (2002).
[35] G. Gantzounis and N. Stefanou, Phys. Rev. B **73**, 035115 (2006).
[36] N. Stefanou and A. Modinos, J. Phys.: Condens. Matter **3**, 8149

(1991).
[37] V. Yannopapas, Phys. Rev. B **75**, 035112 (2007).
[38] A. Modinos, V. Yannopapas, and N. Stefanou, Phys. Rev. B **61**, 8099 (2000).
[39] M. Allard and E. H. Sargent, Appl. Phys. Lett. **85**, 5887 (2004).
[40] J. D. Jackson, *Classical Electrodynamics* (Wiley, New York, 1975).
[41] W. H. Press, S. A. Teukolsky, W. T. Vetterling, and B. P. Flannery, *Numerical Recipes in C* (Cambridge University Press, New York, 1997).
[42] M. Inoue, Phys. Rev. B **36**, 2852 (1987).
[43] Y. Kurokawa, Y. Jimba, and H. Miyazaki, Phys. Rev. B **70**, 155107 (2004).
[44] F. García-Santamaría, J. F. Galisteo-López, P. V. Braun, and C. López, Phys. Rev. B **71**, 195112 (2005).